Available online at www.sciencedirect.com

ScienceDirect

Procedia CIRP 74 (2018) 158–162

www.elsevier.com/locate/procedia

10th CIRP Conference on Photonic Technologies [LANE 2018]

Assessing the predictive capability of numerical additive manufacturing simulations via in-situ distortion measurements on a LMD component during build-up

M. Biegler [a,*], B. Graf [a], M. Rethmeier [a,b]

[a] *Fraunhofer Institute of Production Systems and Design Technology (IPK), Pascalstrasse 8-9 10587 Berlin, Germany*
[b] *Bundesanstalt für Materialforschung und –prüfung (BAM), Unter den Eichen 87, 12205 Berlin, Germany*

* Corresponding author. *E-mail address:* max.biegler@ipk.fraunhofer.de

Abstract

Due to rapid, localized heating and cooling, distortions accumulate in additive manufactured laser metal deposition (LMD) components, leading to a loss of dimensional accuracy or even cracking. Numerical welding simulations allow the prediction of these deviations and their optimization before conducting experiments. To assess the viability of the simulation tool for the use in a predictive manner, comprehensive validations with experimental results on the newly-built part need to be conducted.
In this contribution, a predictive, mechanical simulation of a thin-walled, curved LMD geometry is shown for a 30-layer sample of 1.4404 stainless steel. The part distortions are determined experimentally via an in-situ digital image correlation measurement using the GOM Aramis system and compared with the simulation results. With this benchmark, the performance of a numerical welding simulation in additive manufacturing is discussed in terms of result accuracy and usability.

Peer-review under responsibility of the Bayerisches Laserzentrum GmbH.

Keywords: Laser metal deposition; Directed Energy Deposition; DED; Welding Simulation; Digital Image Correlation; Dimensional Accuracy

1. Introduction

In additive manufacturing (AM) Laser Metal Deposition, 3-dimensional geometries are built by locally welding a wire or powder material onto a substrate or pre-existing geometry [1]. A wide range of materials can be deposited, including titanium alloys and stainless steel [2]. During welding, the pre-existing material is re-heated periodically, creating complex effects such as thermal strains, local melting, phase transformations and annealing. When building large AM-LMD parts such as turbine housings [3] or excavator arms [4], the build is set up experimentally and iterated a number of times for parameter search – with each construction taking hours of machine- and personnel-time – before satisfactory results are achieved. Numerical simulations have the potential to reduce the experimental effort for parameter search, build-planning and shape optimization in AM-LMD by conducting virtual tests before experimental trials. In order to use numerical simulation to reduce the experimental effort, challenges regarding long calculation times, the availability of reliable material data and the difficulty of obtaining reference measurements for validation of the model need to be overcome.

Peer-review under responsibility of the Bayerisches Laserzentrum GmbH.
10.1016/j.procir.2018.08.069

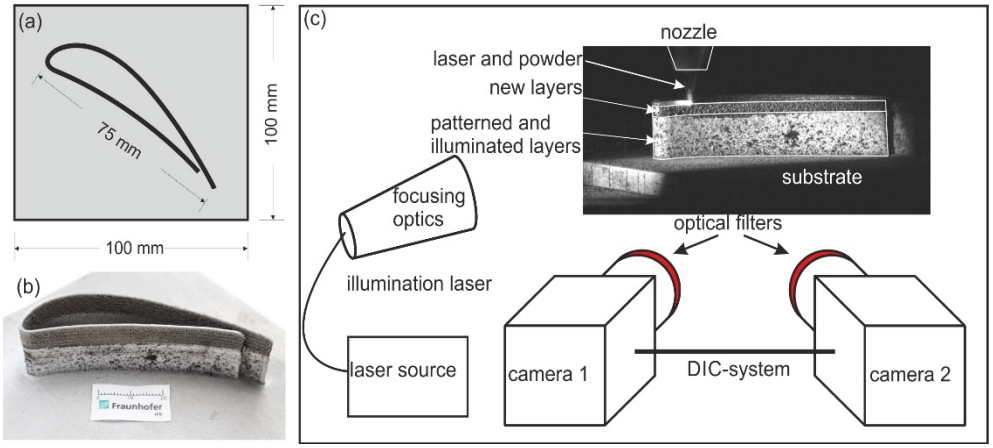

Fig. 1. Experimental setup. Top-down view of the geometry (a). (b): Finished part after buildup of 20 layers, patterning and subsequent 10 layer deposition with DIC measurement. The DIC pattern covering the lower layers is clearly visible. (c): In-situ image with the DIC cameras and the illumination laser sketched in their relative positions during a measurement.

To establish the validity of a numerical simulation model, the calculated temperature flow and development of strains and distortions during build-up and in the finished part are usually compared to experimental data as demonstrated for instance by Perret et al. [5] or Neubert et al. [6] for joint welding. In recent publications, several industrial-scale parts were simulated and compared to experimental results in additive manufacturing using a fully transient simulation approach: Papadakis et al. [3] conducted a structural welding simulation on an aero-engine housing and compared the results to experimental 3D-scans on the finished component. Marimuthu et al. [7] modelled the distortion of the underside in an aero-engine build and compared it to ex-situ coordinate machine measurements. Dunbar et al. [8] also used a coordinate measuring machine to quantify the distortions in selective laser melting (SLM) cylinders. Simunovic et al. [4] simulated the temperature in an excavator arm build. In these publications, the validation measurements are conducted on the final shape, giving a good overview over the quality of the simulation results. As the in-situ measurements are not available, the occurrence of deviations between simulation and experiment cannot be traced, lowering the confidence in the model.

In-situ measurements in LMD are also available, but they usually employ a 1-dimensional laser distance sensor on the underside of a cantilever substrate with a large distance to the newly-built part as shown by Denlinger [9] and Heigel [10] among others. While this generates in-situ measurements, it only quantifies the combined forces of the clad acting on the substrate and does not allow to observe specific effects on the component.

In a recent publication by the authors [11], a novel in-situ measurement method was introduced to quantify distortions directly on a wall sample. 3D-Digital Image Correlation (DIC) was utilized in measurements during the build-up and the experimental results were compared to a structural finite-element simulation. Good agreement of the transient distortions was reported especially for the length direction of the sample but no data for complex cases was shown. In this work, the method established in the prior publication is extended from a simple wall onto a curved, thin-walled AM-LMD component. The formation of displacements in the component are measured using in-situ DIC and subsequently compared to an elasto-plastic FE-model.

2. Methods

A curved, thin-walled AM-LMD geometry was built from 1.4404 stainless steel powder onto a 100x100x6 mm³ 1.4404 substrate plate with the same setup as in [11]. In brief, a coaxial powder nozzle welded single tracks onto one another with 400 W laser beam power, 0.6 mm spot diameter and 7.5 g/min of powder flow. The sample geometry was the curved outline of a turbine blade (Figure 1 a-b). 20 tracks were welded on top of one another with 30 s pause time between layers and a bi-directional strategy, resulting in a wall-thickness of 1.2 mm and a height of 12.4 mm. Then the process was stopped to apply the stochastic pattern required for DIC measurements. Subsequently, 10 additional layers were deposited, while measuring in-situ displacements with the commercial 3D DIC system GOM Aramis 4m. In the optical measurements, the bright process light was blocked with narrow bandpass optical filters, suppressing all wavelengths except 810 nm ± 22.5 nm. A defocused, monochromatic laser was used to illuminate the sample with 808 nm light so that the sample was sufficiently bright for the measurements [12].

The elasto-plastic finite-element simulation was conducted with the same model from [11] in the commercial FE-software simufact.welding 7.1. In a first step, the heat input and thermal boundary conditions (i.e. convection to surrounding air and radiation) were calibrated against a single track thermocouple measurement in order to correctly model the heat input with a mathematical heat source. The calibrated heat source heated and activated the model step by step, matching the progress of the real build for 20 layers. Cooling to room temperature was simulated to conclude the first simulation step as – in the experiment – the DIC pattern was applied. Subsequently, a new model was set-up, keeping the residual stresses and plastic strains from the first step but setting the final distortions to Zero to have the same reference as in the DIC measurement. Afterwards, 10 additional layers were deposited on top and final cooling was simulated. In each increment, the change in geometry, the heat generation

and –spread as well as the thermal strains, displacements and stresses were calculated according to the thermal and mechanical boundary conditions, the model geometry and the residual stresses from the first 20 layers. With a weld length of ~155 mm per layer and a total of 4.65 m for the whole part, the calculation time was 15 h for the first 20 layers and 10.5 h for the 10 topmost layers. The temperature dependent material properties for 1.4404 stainless steel were taken from [13].

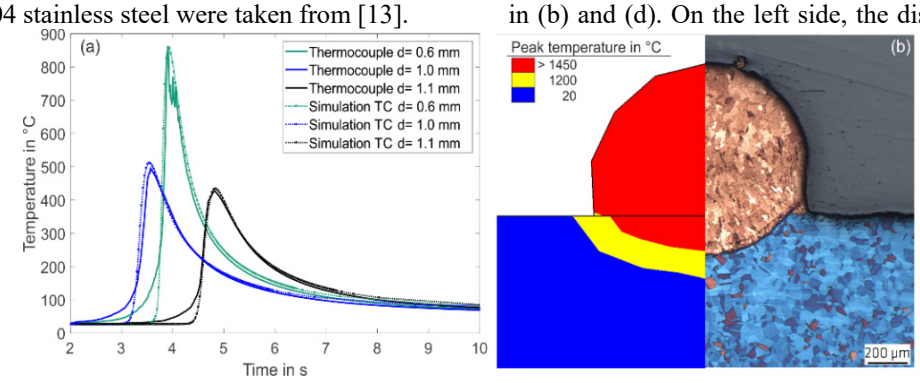

Fig. 2. Comparison of temperatures between experiment and simulations and metallographic cross section with permission from [11]. Three thermocouples were fixed onto the substrate and a single track was welded next to them (a). The simulated and experimental cross sections are compared in (b) with the dark red area in the simulation image and the brown-colored area in the experimental cross-section denoting the molten material during welding.

3. Results and Discussion

The results for the thermal calibration are depicted in Figure 2a, showing a very good agreement between the measured and simulated temperature development. Both the heat input – visible in the peaks – and the thermal conduction and thermal boundaries – visible in the cooling rates respectively – match well for an energy absorption efficiency of 60 % and a convective cooling of 35 W/m²K. In addition, the extent of the molten zone was compared between experimental cross section and the numerical results with good agreement in Figure 2b. With these results, the heat input is considered to match the experiments and will be used as an input in the mechanical model to assess its predictive quality.

The structural finite-element simulation is conducted for the build-process with the validated heat input, the temperature dependent material parameters for 1.4404 as well as the geometry and welding parameters taken from the experiment. Figure 3 compares the y-displacement – i.e. out of plane movement – between experiment and simulation for the first layer at 6 s weld time and for the finished part after 600 s. The scaling is the same across all images. It is well visible, that the geometry bends inwards during welding in (a) and (c) – increasing the radius of curvature – and bends outwards –decreasing the radius of curvature – after welding in (b) and (d). On the left side, the displacements are smaller because of the stiffness of the small-radius curvature, whereas the right side is free to deform without additional stiffness. The experiment and simulation both depict this behavior with the calculated displacements matching the experimental results in quality and quantity. The graphics in Figure 3 show a two-dimensional displacement at a single time step each but to utilize the full potential of the in-situ measurements and of the transient simulation results, time-dependent displacements can be compared. In Figure 4, the time-dependent displacements for x-, y- and z-displacements at P1 (Figure 3) are compared between DIC and FEA. For the experimental results, a small standard deviation from three repetitions is visible in y- and z-displacements, proving the reliability of the DIC method. In the y-displacements, a periodic inward bending and outward shrinking in agreement with the surface plots in Figure 3 is observed. With each layer, the geometry deforms, steadily adding up a lasting displacement. After cooling, the residual y-displacement exhibits a magnitude of about 0.22 mm both in simulation and experiment. In z-direction the same layer-wise expansion and shrinkage is

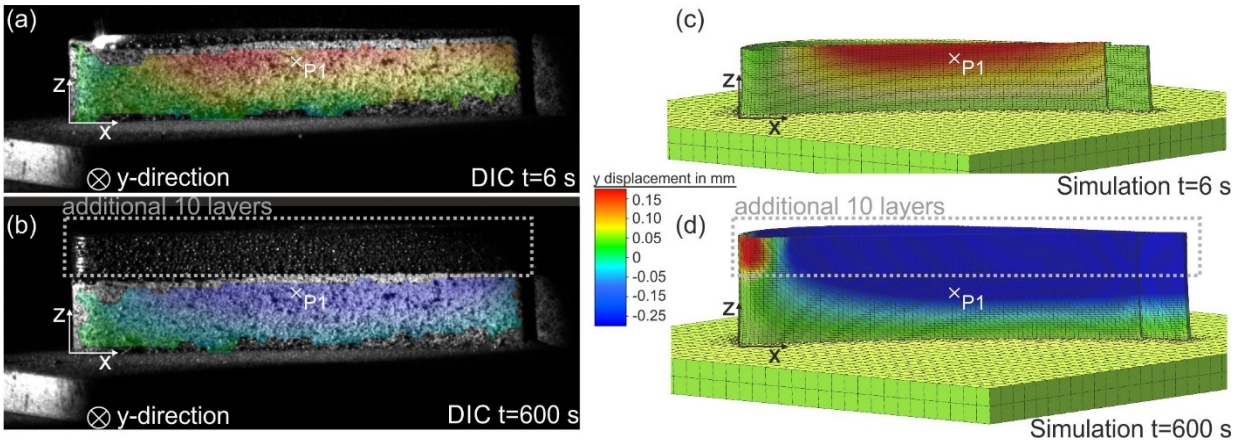

Fig. 3. Comparison of experimental (a-b) and simulated (c-d) y-displacements at 6 s welding time and after finishing the part with 10 additional layers. The experimental and simulated displacements show an inward bending during welding and an outward (towards the viewer) shrinking after cooling. In (d) the availability of results across the whole component is visible for the simulation, whereas the DIC measurement (b) is limited to the pre-patterned surface.

visible, however little permanent displacement is added up as the deformations appear to be mainly elastic. Because the measured values are very small for the x-displacement, the scatter is comparatively large and both for simulation and experiment, displacements in this direction are almost nonexistent in the middle of the curved wall-geometry.

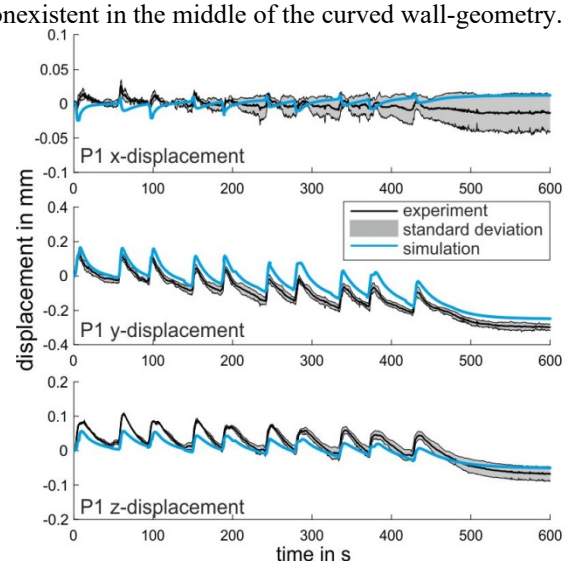

Fig. 4. Comparison of the transient displacement in x-, y- and z-directions at P1 (Fig. 3.) between experiment and simulation.

The absence of in-plane displacements in the middle of the geometry is comparable to the DIC results for the wall in [11]. There, the x-displacements are only pronounced at the edges of the wall, bending outwards during welding and shrinking inwards during cooling. For the y-displacement, no in-situ results are available in the literature to the author's knowledge. The wall studied before did not exhibit any out-of-plane motion because it was not curved and no other study measured the displacements during welding in AM-LMD. However, the residual distortion for a curved part after welding were measured in several studies and can be compared to the results: In the engine-housing from Papadakis et al. [3], a comparable bending is observed for the component at 10 mm height from the substrate. Dunbar et al. [8] determined a similar shrinking for selective laser melting cylinders with a coordinate measuring machine. With this comparison, a good agreement between experiment, simulation and the distortions reported in the literature was shown.

4. Conclusion

In this work, a recently established setup for 3-dimensional in-situ distortion measurements in AM-LMD geometries was applied to an arbitrarily curved part. The method generated well-reproducible results for transient x-, y- and z-distortions. The most pronounced distortion was y-distortion: with each layer, the displacements added up, leading to a shape deviation of about 0.22 mm after 10 layers.

The data was subsequently used to validate a thermomechanical simulation model. After calibration of the heat input, the in-situ displacements were calculated for the whole build and showed very good agreement in quality and quantity with the experimental results.

As the predictive quality of the model has been tested, it can now be used to calculate data, where no experimental measurements is possible – i.e. for the layers without DIC pattern or for the other side of the part. In order to extend the model to different parts, the calibration of the heat input has to be re-done for new parameters and the track thickness and width has to be adjusted to match the experiment. To reduce calculation times for larger parts, simplifications such as layer-wise heating or mechanical surrogate models could be used instead of the transient heat-input model. In order to test the validity of simplifications, the extensive in-situ data gathered for this study could be re-used in the future.

Acknowledgements

The IGF-project 18737 N of the research association Forschungsvereinigung Stahlanwendung e.V. (FOSTA), Sohn-straße 65, 40237 Düsseldorf, was funded through the AiF within the program of the promotion of the industrial joint research (IGF) by the Federal Ministry for Economic Affairs and Energy based on a resolution of the Deutsche Bundestag.

References

[1] W. E. Frazier, "Metal Additive Manufacturing: A Review," *J. of Materi Eng and Perform*, vol. 23, no. 6, pp. 1917–1928, 2014.

[2] B. Graf, A. Gumenyuk, M. Rethmeier, "Laser Metal Deposition as Repair Technology for Stainless Steel and Titanium Alloys," *Physics Procedia*, vol. 39, pp. 376–381, 2012.

[3] L. Papadakis and C. Hauser, "Experimental and computational appraisal of the shape accuracy of a thin-walled virole aero-engine casing manufactured by means of laser metal deposition," *Prod. Eng. Res. Devel.*, vol. 11, no. 4-5, pp. 389–399, 2017.

[4] S. Simunovic, A. Nycz, M. Noakes, C. Chin, V. Oancea, "Metal Big Area Additive Manufacturing: Process Modeling and Validation," *NAFEMS World Congress 2017*, 2017.

[5] W. Perret, R. Thater, U. Alber, C. Schwenk, M. Rethmeier, "Approach to assess a fast welding simulation in an industrial environment — Application for an automotive welded part," *Int.J Automot. Technol.*, vol. 12, no. 6, pp. 895–901, 2011.

[6] S. Neubert, A. Pittner, M. Rethmeier, "Influence of non-uniform martensitic transformation on residual stresses and distortion of GMA-welding," *Journal of Constructional Steel Research*, vol. 128, pp. 193–200, 2017.

[7] S. Marimuthu, D. Clark, J. Allen, Am Kamara, P. Mativenga, L. Li, R. Scudamore, "Finite element modelling of substrate thermal distortion in direct laser additive manufacture of an aero-engine component," *Proceedings of the Institution of Mechanical Engineers, Part C: Journal of Mechanical Engineering Science*, vol. 227, no. 9, pp. 1987–1999, 2012.

[8] A. J. Dunbar, E. R. Denlinger, M. F. Gouge, P. Michaleris, "Experimental validation of finite element modeling for laser powder bed fusion deformation," *Additive Manufacturing*, vol. 12, pp. 108–120, 2016.

[9] E. R. Denlinger and P. Michaleris, "Effect of stress relaxation on distortion in additive manufacturing process modeling," *Additive Manufacturing*, vol. 12, pp. 51–59, 2016.

[10] J. C. Heigel, M. F. Gouge, P. Michaleris, T. A. Palmer, "Selection of powder or wire feedstock material for the laser cladding of Inconel ® 625," *Journal of Materials Processing Technology*, vol. 231, pp. 357–365, 2016.

[11] M. Biegler, B. Graf, M. Rethmeier, “In-situ distortions in LMD additive manufacturing walls can be measured with digital image correlation and predicted using numerical simulations,” *Additive Manufacturing*, vol. 20, pp. 101–110, 2018.
[12] N. Bakir, A. Gumenyuk, M. Rethmeier, “Investigation of solidification cracking susceptibility during laser beam welding using an in-situ observation technique,” *Science and Technology of Welding and Joining*, vol. 7, pp. 1–7, 2017.
[13] J. J. Janosch, *IIW Round Robin protocol for residual stress and distortion prediction, Phase II (Proposal Rev. 1), IIW Doc. X/XV-RSDP-59-00*, 2000.